3B2v8.06a/w (Dec 5 2003).51c +model NEUCOM : 10288 Prod.Type:FTP pp.1–8(col.fig.:NIL) ED:BabuB. PAGN:NMN SCAN:prasanth

Available online at www.sciencedirect.com

SCIENCE DIRECT®

Neurocomputing ▮ (▮▮▮▮) ▮▮▮–▮▮▮

NEUROCOMPUTING

www.elsevier.com/locate/neucom

A computational model of anterior intraparietal (AIP) neurons

Erhan Oztop[a,b,*], Hiroshi Imamizu[b], Gordon Cheng[a,b], Mitsuo Kawato[a,b]

[a] *JST-ICORP Computational Brain Project*

[b] *ATR Computational Neuroscience Laboratories, Department of Cognitive Neurosciences, 2-2-2 Hikaridai, Soraku-gun Seika-cho, Kyoto 619-0288, Japan*

Abstract

The monkey parietal anterior intraparietal area (AIP) is part of the grasp planning and execution circuit which contains neurons that encode object features relevant for grasping, such as the width and the height. In this study we focus on the formation of AIP neurons during grasp development. We propose and implement a neural network structure and a learning mechanism that is driven by successful grasp experiences during early grasp development. The simulations show that learning leads to emergence of units that have similar response properties as the AIP visual-dominant neurons. The results may have certain implications for the function of AIP neurons and thus should stimulate new experiments that cannot only verify/falsify the model but also advance our understanding of the visuomotor learning mechanisms employed by the primate brain.

© 2006 Published by Elsevier B.V.

Keywords: Anterior intraparietal area; Grasp learning; Affordance; Visuomotor development

UNCORRECTED PROOF

1. Introduction

Humans visually monitor critical kinematic events for detecting errors in goal-directed movement execution [8] including grasping movements that require cortical integration of visual and somatosensory cues for proper grip formation [6]. The accumulated neurophysiological data indicate that the parietal cortex is involved in visuomotor aspects of manual manipulative movements [19]. In particular, the neurons in anterior intraparietal (AIP) area of macaque monkeys discharge in response to viewing and/or grasping of three-dimensional objects representing object features relevant for grasping [14,16]. Generally, AIP neurons are classified as one of motor-dominant (active during grasping, even in the dark), visual-motor, and visual-dominant (no movement is necessary; sole object fixation elicits response) types. AIP has strong recurrent connection with area F5 (ventral premotor cortex) [10] that is involved in grasp planning and execution [13], and projects to motoneurons that control finger muscles [2]. The activity of neurons in the primary motor cortex (F1) when compared to premotor activity indicates that the primary motor cortex may be more involved in dynamic aspects of movement [18], executing 'instructions' sent by higher motor centers including premotor regions. Thus, it has been suggested that AIP–F5–F1 circuit is responsible for grasp planning and execution [3–5,7]. However the formation/adaptation of the neural circuitry that extracts object features required for dexterous manipulation (i.e. AIP) is yet to be understood. To this end, it is important to know whether AIP representation is the final step of a series of visual analysis or the by product of the grasp-related visuo-motor learning.

In this article, we present a model of AIP visual-dominant neurons consistent with monkey grasping circuit that extends upon our earlier modeling of infant grasp learning (when we use AIP, we mean AIP visual-dominant from now on). Infant motor development studies have shown that during early grasping period of 4–6 months, infants do not use vision to guide hand trajectory or to orient the hand toward the object prior to initial contact.

*Corresponding author. ATR Computational Neuroscience Laboratories, Department of Cognitive Neurosciences, 2-2-2 Hikaridai, Soraku-gun Seika-cho, Kyoto 619-0288, Japan. Tel.: +81 774 95 1215; fax: +81 774 95 1236.

E-mail addresses: erhan@atr.co.jp (E. Oztop), imamizu@atr.co.jp (H. Imamizu), gordon@atr.co.jp (G. Cheng), kawato@atr.jp (M. Kawato).

0925-2312/$ - see front matter © 2006 Published by Elsevier B.V.
doi:10.1016/j.neucom.2005.12.106

For example, at 4–5 months, reaches are as good with vision available during the reach as when vision is removed after onset of the reach [1]. Only after 9 months of age the visual features of the objects that are relevant for grasping (orientation, size, etc.) are incorporated into the grasping actions. This developmental progression suggests that earlier grasp learning may mediate the formation of a stronger grasp planning circuit that fully utilizes the visual information available. The model we present addresses the latter portion of this progression, where the less-visually guided grasp experiences provide (learning) data points for an infant's grasp related visuo-motor mapping system.

2. The model

2.1. Behavioral setting

The model we present addresses the developmental stage of 4–9 months where a basic grasping skill has been acquired. We present the model in terms of brain areas belonging to macaque monkeys, however, the developmental data is mainly from humans due to the lack of infant studies on other primates. In other words, we implicitly assume that the developmental aspects of the grasp circuit in humans and other primates follow similar stages.

The grounding assumption of the modeling presented in this article is that during early grasp learning infants associate the vision of the objects with the grasp plan (the motor code generating the grasp) that provides a stable grasping.

2.2. The systems level organization

We abstract the primate grasping circuit as shown in Fig. 1A. The visual input arriving to AIP—although processed at earlier visual areas—is void of geometric information about the object in the visual field. The task of AIP–F5 complex is then to transform the visual input into a motor code which when executed yields a successful (stable) grasping of the object. In the primates, the input to AIP is highly processed as there are multiple relay stations on the way from primary visual cortex to AIP. Nevertheless, these areas do not compute information such as width and height of the object in the visual field. To our knowledge, AIP and caudal intraparietal sulcus (cIPS) are the sole areas reported to encode geometric object properties. cIPS neurons encode orientation or axis of objects and may provide information for AIP [15]. For simplicity we do not model cIPS explicitly as a separate layer. However, we do expect to see units similar to cIPS neurons as well in our AIP layer (in spite of the naming). For this article, we focus only on the properties of unit responses that are comparable to AIP-like responses.

2.3. Input and output encoding

To capture the non-specificity of the visual input (i.e. lack of geometric information coding) we implemented the input to AIP as a depth encoding 'retina'. The visual processing taking place prior to AIP includes stereopsis, so this choice is justified by the monkey neurophysiology [15]. The most notable point of our representation is that it does not include any high level features extracted by a preprocessing step; what the network sees is just a depth map (i.e. matrix of real numbers). Notice that instead of an explicit depth encoding it is also possible to use two intensity coding retinas corresponding to two eyes, in which case we would predict the emergence of binocular neurons in the hidden layers. Since the depth encoding retina chosen for computational convenience does not contain more information than the two retina system (given the simple objects we used) the validity of the arguments we might draw from the model is not weakened by our choice.

For the motor code (F5) output we used joint angles of the fingers. Although the motor code in the brain must address dynamics and intrinsic properties of the muscles and lower motor control centers we believe the output code used does not limit the validity of the conclusions we can draw from the model.

2.4. Adaptation mechanism

The problem an infant faces during grasp learning is computationally stated as to learn the mapping from visual ($\vec{V}$) to motor codes ($\vec{G}$) that yield successful grasping. Notice that the learning mentioned here is only possible with the active movements of an infant, although the resulting neural structure may exhibit purely visual responses not requiring movement. The infant experiences many $\{\vec{V}_{\mathrm{i}}, \vec{G}_{\mathrm{i}}\}$ pairs during early grasping. At first, this problem seems to assume a simple function approximation solution, however, the mapping is not well defined: we can apply different grasps to a given object. Conversely, different objects can serve as the target for the very same grasp. The problem can be approached from several directions. One way is to model the association learning as learning the joint probability distribution $p(\vec{V}, \vec{G})$ of the visual representation of the object and the motor command. In this study we chose a more biological approach and propose a neural circuit with explicit neural units that can solve the problem: we propose that AIP–F5 complex consists of sub-networks (columns) that compete in the motor code space for being the one to learn the current $\{\vec{V}_{\mathrm{i}}, \vec{G}_{\mathrm{i}}\}$ (successful grasp association) pair (see Fig. 1B). The competition is implemented using a Kohonen's topology preserving self-organizing map (SOM). When a grasping attempt results in successful holding of the target object, the competition picks a sub-network to learn the current observed vision$\rightarrow$motor association. Although other alternatives were possible, the learning in the sub-

UNCORRECTED PROOF

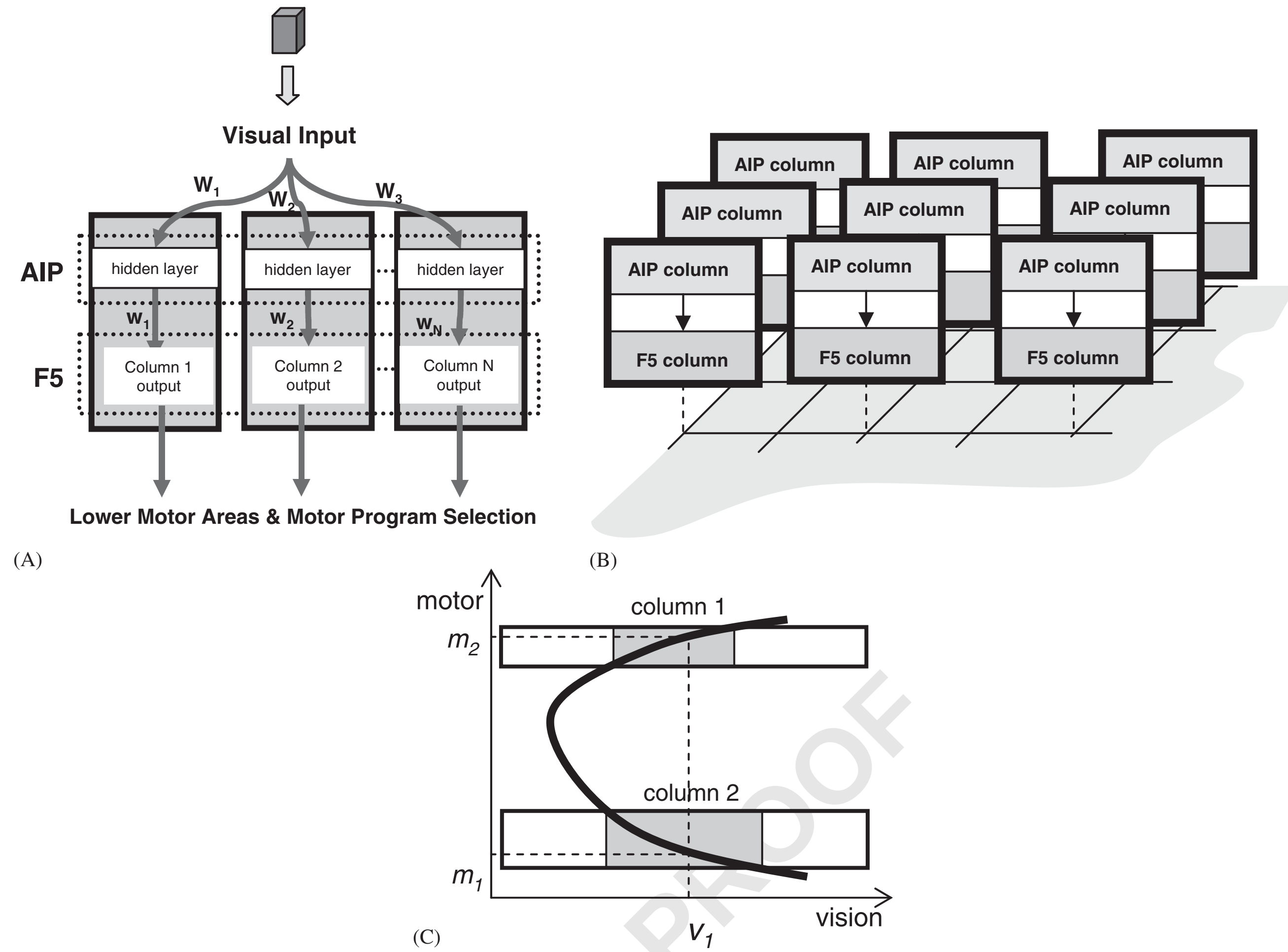

Fig. 1. (A) Overall network representation is shown. The arrows labelled with **W** and **w** indicates the adaptive weights. (B) Competition among AIP–F5 columns (sub-networks) for learning the association of the current vision and the executed grasp code is depicted. (C) Conceptual illustration of how an ill-defined vision → motor relation (the curve) can be learned using multiple columns. A single neural network cannot learn this mapping because $v1$ maps to both $m1$ and $m2$. The strips drawn over the curve symbolically indicate the areas where the columns (sub-networks) become winner for the indicated range of motor values. In these strips the mapping is well-defined (see the curve segments in the shaded areas).

UNCORRECTED PROOF

networks was implemented using back-propagation learning algorithm for computational convenience. The SOM clustering groups similar (in the hand configuration space) grasps together and hence creates sub-problems each of which can be solved with a simple function approximator allowing the sub-networks to learn their sub-problems. This is conceptually illustrated in Fig. 1C where the curve represents a hypothetical vision → motor relation. Notice that at vision $= v1$, the motor output can be either m1 or m2. When a function approximator is used to learn this relation it will be forced to learn conflicting data points, namely ($v1$, $m1$) and ($v1$, $m2$). Since the function approximator can give only single output for the input of $v1$, the learning will not be able to reduce the prediction error to zero (see also [9]). However, if the curve was cut into horizontal stripes then within each stripe the relation would be learnable (see the shaded regions in Fig. 1C). This is exactly what the self-organization in the motor space does; it partitions the motor space such that in a given partition, the vision → motor relation becomes well defined. This scheme works provided that the number of sub-networks is sufficient enough to accommodate the number of sub-problems required to reduce the association problem into a set of well defined $\vec{V}_\mathrm{i} \rightarrow \{\vec{G}_\mathrm{i}\}$ mappings.

2.5. Learning details

Given the successful grasp configuration $\vec{G}_\mathrm{i}$, The SOM update rule used was $\Delta\vec{r}_k = \mu e^{-\Lambda(k^*,k)/\delta^2}(-\vec{r}_k + \vec{G}_\mathrm{i})$ where $\vec{r}_k$ represents the kth sub-network's preferred grasp configuration, and k^* is the winner sub-network. The neighborhood function $e^{-\Lambda(k^*,k)/\delta^2}$ was determined by taking $\Lambda(k^*, k)$ as the Euclidean distance between the 2D *indexes* of sub-networks k and k^*, and setting the variance as $\delta^2 = 2$. In all simulations, the update rate of the SOM was $\mu = 0.001$, and the variance was reduced at each time step by 10^{-6} of the current value of the variance.

For a given (visual-input, grasp configuration) data point ($\vec{V}_i, \vec{G}_i$), the weights of the winner sub-network was updated using a straightforward gradient descent update rule (i.e. back-propagation) on the error $E = 0.5\|\vec{\zeta} - \vec{G}_i\|^2$ where $\vec{\zeta}$ represents the output generated when the input $\vec{V}_i$ was presented. The output $\vec{\zeta}$ was computed with $\vec{\zeta} = f(\mathbf{W}f(\mathbf{w}\vec{V}_i))$, where $f(.)$ is the sigmoid function given by $f(x) = (1 + e^{-x})^{-1}$. Note also that for the operation of this network the input and outputs were normalized to be within the range of [0, 1]. The visual-input→AIP weight matrix ($\mathbf{W}$) was updated with $\Delta\mathbf{W}^t = -\eta\frac{\partial E}{\partial \mathbf{W}} + \beta\Delta\mathbf{W}^{t-1}$, and the AIP→output weight matrix ($\mathbf{w}$) was updated with $\Delta\mathbf{w}^t = -\eta\frac{\partial E}{\partial \mathbf{w}} + \beta\Delta\mathbf{w}^{t-1}$, where η and β represents the learning rate and the coefficient of momentum term, respectively. The superscripts indicate the update step number, so $t-1$ means the previous update step. All of the simulations reported in this article used $\eta = 0.05$ and $\beta = 0.6$.

3. Simulations

The visual input ($\vec{V}$) was modeled as a 32×32 depth map centered on the target object. The motor command ($\vec{G}$) was modeled as the joint configuration of the hand. We used 7 joints: 3 joints for the thumb, 2 joints for the index and middle fingers. The number of sub-networks was 16, and each had 16 or 8 hidden (AIP) units. For the SOM, we used a planar (two dimensional) mesh. The number of nodes was equal to the number of sub-networks (16), and the input dimension was equal to the motor output (7). For input, we used three objects with variable dimensions. The objects were: a rectangular prism (box) which could change size in two dimensions; a vertical cylinder (vertical bar) that could change in height and diameter; and finally a horizontal cylinder (horizontal bar) with variable height and diameter (Fig. 2, right side).

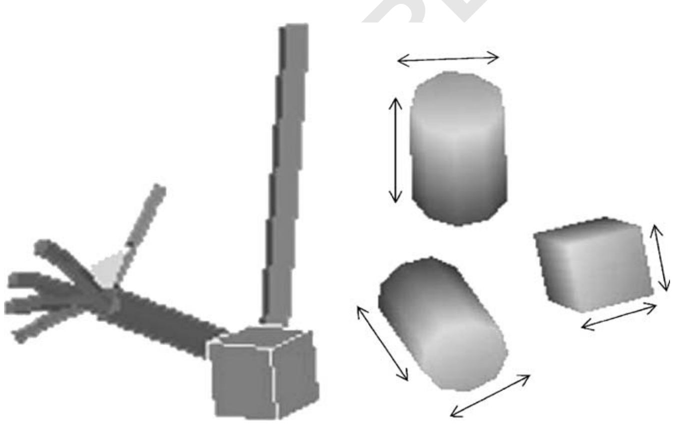

Fig. 2. Grasp learning system that provided successful grasps and corresponding joint angles (left), and the depth map representation used as the input to the model for various objects are shown (right). The arrows indicate the dimensions of the objects that were varied during grasp learning.

As mentioned previously, the current model addresses the stage of motor development where a basic grasping ability is assumed. Our earlier study of infant grasp learning provided us the stage required. We used our implementation of infant grasping learning model (ILGM) [12] to acquire the skill of grasping the aforementioned objects with different sizes (Fig. 2, left side shows the ILGM simulation environment). The successful grasps executed by ILGM then were used to drive the AIP model presented in this article. In ILGM the objects were modeled as 3D geometric shapes, which required us to convert them into depth maps so that they could be fed to AIP. This conversion is performed by rendering the objects into a 32×32 buffer such that the intensity of a rendered pixel indicated its depth as shown in Fig. 2, right side.

We used 2000 successful grasping performances from ILGM to test the AIP model. In those grasping movements the object sizes and types were (uniform) randomly selected. Note that the grasp plan generation mechanism in ILGM is stochastic and produces different grasp configurations at different instances of an object's presentation (even when the dimensions are fixed). Technically, we could implement AIP model on top of ILGM model and run them together, but for practical reasons we kept the two systems separate. We first collected 2000 grasping data points (joint configuration of the hand and the depth map of the grasped objects) and then used them in adapting our model. For the simulations reported in this paper we applied a sequential training schedule: first the SOM was adapted, then each sub-network was allowed to learn for those grasp codes that they became winner for. The learning was stopped after all the sub-networks had converged. The norm of the error was ~0.45 for the 8 AIP unit case, and ~0.4 for the 16 AIP unit case. This corresponds approximately to an average of ~6 and ~5 degrees of error per finger joint angle, respectively.

4. Results

After learning has converged, we presented the objects with varying dimensions recording the elicited response at each of the AIP units. Since two dimensions of the objects were altered, a given object provided us with a two-dimensional mesh of response values (called the response map) for each unit. Before presenting the actual response maps of the units we briefly report the *object encoding* emerged via learning using 16 AIP units per sub-network [8 AIP units per sub-network]: for each object type we listed all the units that have higher activity than in all other object presentations by a margin of ~0.1 [~0.05] (remember that maximal firing is 1.0). Interestingly, number of selective units for each object was more or less the same for each object (i.e. the list contained approximately the same number of units). Approximately, 8 [4] out of 256 [128] units became selective for each object (box, horizontal bar, and vertical bar). And of those only 1 or 2 [1 or none] units were strictly selective for a specific size of the object.

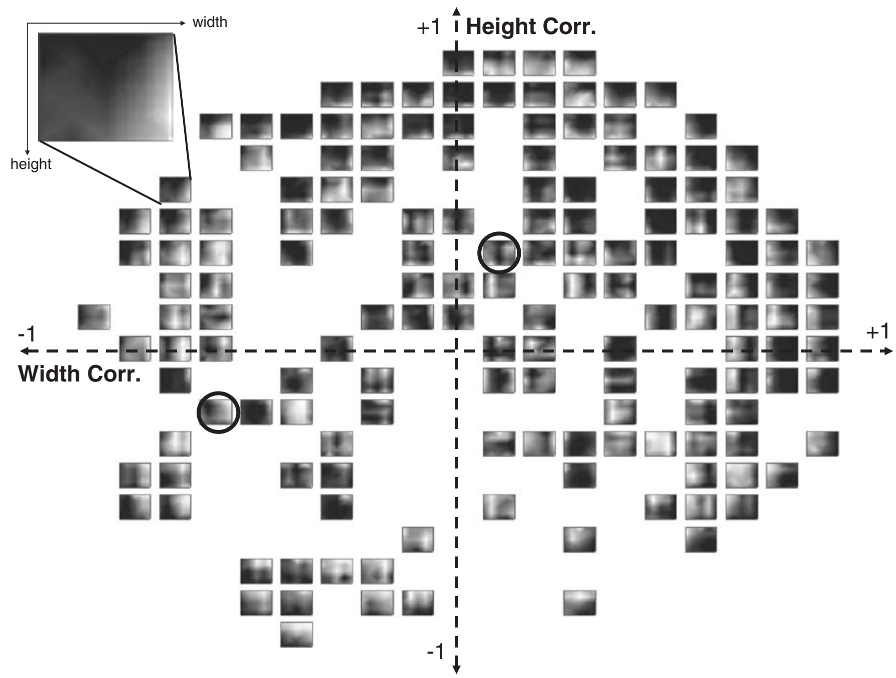

Fig. 3. Response of AIP units (after learning) when the box object was presented with varying width and height values (number of AIP units per sub-network = 16). The thumbnail images (response maps) indicate the AIP units' response to the varying width and height values of the box. The darker areas indicate higher response, whereas lighter areas indicate smaller response. The magnification on the top left shows the axes of the response maps. The location of a unit's response map shows the feature encoding by that unit: the ones on the left and right extremes have responses that correlate well with the width of the presented box. Similarly, the units on the upper and lower extremes have responses that correlate well with the height of the presented box. Note that although there are 256 AIP response maps, because of the special arrangement of the response maps, some overlapped (because they had close correlation values for the width and height).

UNCORRECTED PROOF

In order to visually inspect the response map of units we have created image maps (small thumbnail images) in which darker regions indicate higher response, while white regions indicate zero response, as shown in Fig. 3. A vertical gradation in the intensity indicates that the unit encodes the height of the object, whereas a horizontal gradation indicates a width encoding. For space limitations we can only present the response maps obtained from the presentation of one object (box) using the 16 AIP units per sub-network (Fig. 3). The location of each response map was specially chosen: the position of the response maps within the drawn axes, indicate the level of geometric feature encoding of units: the horizontal axis indicates the correlation of unit response with the width of the box, where as the vertical axis indicates the correlation of unit activity with the height of the box. Therefore, the units at the left and right extremes encode the width of the box, whereas the units at upper and lower extreme encode the height. The units around the origin do not have a clear (linear) correlation with the dimensions of the box. Note that there are units which encode a certain range of width or height, one example is marked in the first quadrant with a circle. In addition, there are a few units that prefer certain width and height in combination; the unit marked in the third quadrant, for example, prefers small boxes. These types of units are rarer than the width and height encoding units and are located away from the $+1$ and -1 in the correlation axes as these units do not have a *linear* correlation with the object dimensions. The sigmoidal network we used is characterized by the non-local basis functions implemented by the hidden layers, which are formed via training [17]. It could be speculated that the variety of neural responses we obtained could be attributed to this fact. If we used local learning networks (i.e. radial basis function network) the neural responses might have been more stereotypical, having convex shaped high-response areas when plotted as in Fig. 3.

Because of space limitations we revert to simple scatter plots for presenting the responses of the AIP units for other objects. In Fig. 4, each unit is indicated by a triangle; the horizontal axis indicates the *absolute value* of the linear correlation of unit responses with the horizontal extent of the object presented. Likewise, correlation with the vertical extent is represented on the vertical axis. Row A indicates the objects used in computing the correlations. The last column of Fig. 4A indicates that all of the objects were considered in the correlation computation illustrating the emergence of units with size encoding *independent of object identity*. Row B shows the results obtained when the number of AIP units was set to 8 per sub-network, whereas Row C shows the results when the number of AIP units was 16. Comparing Row B and C we can see that the

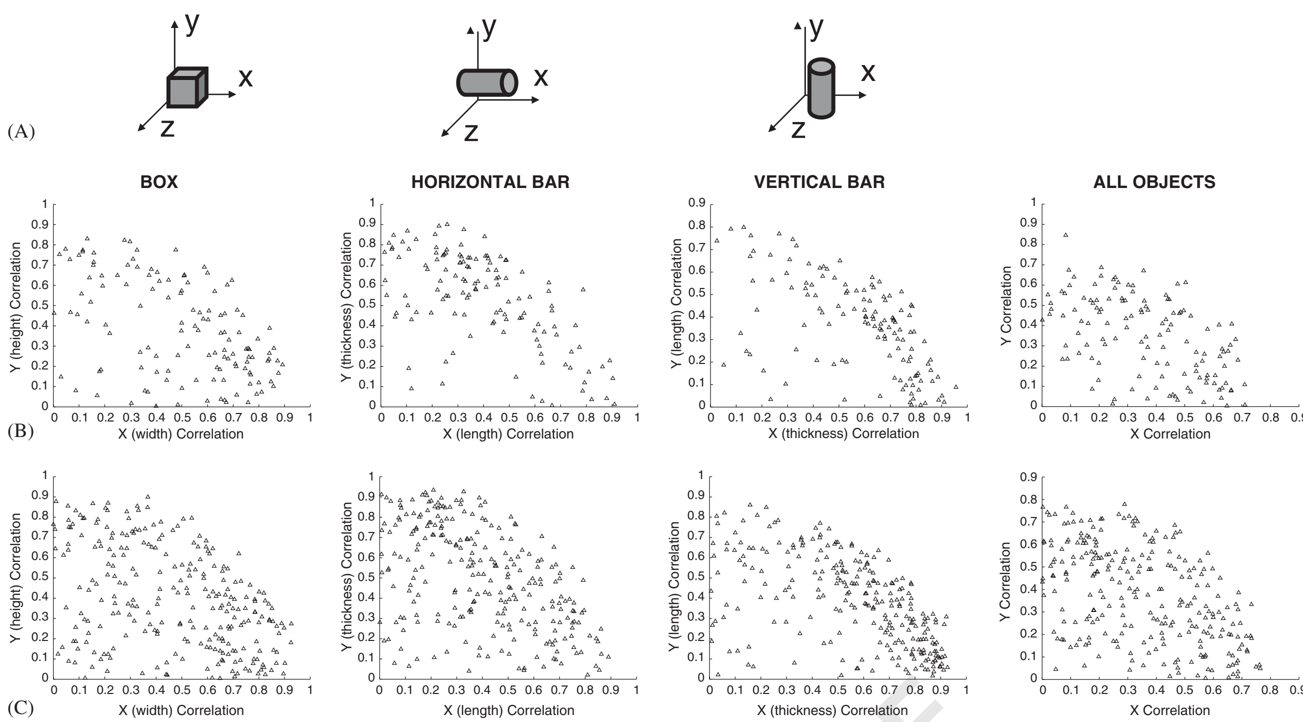

Fig. 4. (A) Objects presented for computing the correlations that are shown in the lower rows. (B) Correlation results when the sub-networks were modelled with 8 AIP units. (C) Results are shown when the number of the AIP units was increased to 16. Each triangle represents an AIP unit, where the coordinates of a unit represents its (absolute valued) correlation with the indicated object dimension. So the units that have coordinates close to 1 can be said to represent geometric features of the presented objects.

distribution of units have strong similarity even though they were obtained through different simulations with different number of AIP units.

5. Conclusion

The monkey AIP has neurons with complex visuo-motor properties. Some of them are mainly activated during grasp execution whereas others can be activated by mere visual fixation of the objects (visual-dominant object-type neurons) [15]. The current model addresses the latter type of neurons that become active even though no subsequent movement is involved. In literature, a range of object selectivity has been reported for the object-type neurons; a highly selective neuron shows vigorous activity to a single object and responds weakly to other objects, whereas, a broadly selective neuron may respond to more than one object, often which have similar geometric features [11]. The simulation experiments with our model showed that units with a range of object selectivity can emerge via visuo-motor learning. Most of the units we have found were broadly tuned showing response to more than one object type. This is consistent with the experimental studies that report that the number of AIP neurons with strict selectivity is less than the broadly selective neurons [11].

With the goal of stimulating new experimental studies, the main focus of the current modeling study was to test whether *size selectivity* could emerge from visuo-motor learning. As presented in results, we have found units that encode object dimensions (some with independent of the object shape). Indeed, it has been reported that many neurons found in monkey AIP were selective for the size and the shape (often in conjunction) of the objects being viewed [11]. However to our knowledge, there is no experimental study to show that AIP neurons represent geometric *quantities* (i.e. measure of say, thickness rather than the attributes of thin/thick). The results from our simulations suggest that if AIP visual-dominant neurons are part of a visuo-motor grasp learning network, as is usually accepted [7,16], then (1) shape and size selectivity emerges naturally via learning, and furthermore (2) the phrase ‘shape and size selectivity’ can be replaced with ‘representation of geometric features’, or better with ‘representation of affordances for grasping’. It is possible to test the latter implication of our model with further neurophysiological experiments that involve systematic size alterations of the presented objects to the subject monkey, allowing a reliable correlation analysis on the recorded data.

An unanswered question by the presented model is how the two learning systems interact. The model predicts that during the early phases of infant grasping, output from the visuo-motor circuit would not be accurate (due to e.g. lack of sufficient learning data points). Therefore if the infants have no complete control to suppress this inaccurate output, the vision of the detailed shape of the object must

UNCORRECTED PROOF

degrade the grasping performance. The closest experimental findings to our prediction indicates that 3 months old infants reach for and contact with glowing and sounding objects under lighted and dark conditions with similar frequency, and the onset of successful grasping occurs at approximately at the age of 15–16 weeks for both conditions [1]. This means that 3 months old infants do not take advantage of the visibility of the shape of the object. Perhaps with more strict experimental conditions it might be possible to show that at the age of 3–4 months, the object shape information in fact degrades the grasping performance.

Acknowledgments

This work was supported by JST-ICORP Computational Brain project. We thank Akira Murata for useful discussions.

References

[1] R.K. Clifton, D.W. Muir, D.H. Ashmead, M.G. Clarkson, Is visually guided reaching in early infancy a myth?, Child Dev. 64 (1993) 1099–1110.

[2] R.P. Dum, P.L. Strick, The origin of corticospinal projections from the premotor areas in the frontal lobe, J. Neurosci. 11 (1991) 667–689.

[3] A.H. Fagg, M.A. Arbib, Modeling parietal–premotor interactions in primate control of grasping, Neural Networ. 11 (1998) 1277–1303.

[4] L. Fogassi, V. Gallese, G. Buccino, L. Craighero, L. Fadiga, G. Rizzolatti, Cortical mechanism for the visual guidance of hand grasping movements in the monkey—a reversible inactivation study, Brain 124 (2001) 571–586.

[5] V. Gallese, A. Murata, M. Kaseda, N. Niki, H. Sakata, Deficit of hand preshaping after muscimol injection in monkey parietal cortex, Neuroreport 5 (1994) 1525–1529.

[6] M. Jeannerod, The formation of finger grip during prehension. A cortically mediated visuomotor pattern, Behav. Brain Res. 19 (1986) 99–116.

[7] M. Jeannerod, M.A. Arbib, G. Rizzolatti, H. Sakata, Grasping objects—the cortical mechanisms of visuomotor transformation, Trends Neurosci. 18 (1995) 314–320.

[8] R.S. Johansson, G. Westling, A. Backstrom, J.R. Flanagan, Eye–-hand coordination in object manipulation, J. Neurosci. 21 (2001) 6917–6932.

[9] M.I. Jordan, D.E. Rumelhart, Forward models—supervised learning with a distal teacher, Cognitive Sci. 16 (1992) 307–354.

[10] M. Matelli, G. Luppino, A. Murata, H. Sakata, Independent anatomical circuits for reaching and grasping linking the inferior parietal sulcus and inferior area 6 in macaque monkey, in: Society for Neuroscience, vol. 20, 1994, p. 404.

[11] A. Murata, V. Gallese, G. Luppino, M. Kaseda, H. Sakata, Selectivity for the shape, size, and orientation of objects for grasping in neurons of monkey parietal area AIP, J. Neurophysiol. 83 (2000) 2580–2601.

[12] E. Oztop, N.S. Bradley, M.A. Arbib, Infant grasp learning: a computational model, Exp. Brain Res. 158 (2004) 480–503.

[13] G. Rizzolatti, M. Gentilucci, R.M. Camarda, V. Gallese, G. Luppino, M. Matelli, L. Fogassi, Neurons related to reaching—grasping arm movements in the rostral part of area-6 (area-6a-beta), Exp. Brain Res. 82 (1990) 337–350.

[14] H. Sakata, M. Taira, M. Kusunoki, A. Murata, Y. Tanaka, K. Tsutsui, Neural coding of 3D features of objects for hand action in the parietal cortex of the monkey, Philos. Trans. Roy. Soc. London Series B-Biol. Sci. 353 (1998) 1363–1373.

[15] H. Sakata, M. Taira, M. Kusunoki, A. Murata, K. Tsutsui, Y. Tanaka, W.N. Shein, Y. Miyashita, Neural representation of three-dimensional features of manipulation objects with stereopsis, Exp. Brain Res. 128 (1999) 160–169.

[16] H. Sakata, M. Taira, A. Murata, S. Mine, Neural mechanisms of visual guidance of hand action in the parietal cortex of the monkey, Cereb. Cortex 5 (1995) 429–438.

[17] S. Schaal, C.G. Atkeson, Constructive incremental learning from only local information, Neural Comput. 10 (1998) 2047–2084.

[18] L.M. Shen, G.E. Alexander, Preferential representation of instructed target location versus limb trajectory in dorsal premotor area, J. Neurophysiol. 77 (1997) 1195–1212.

[19] S.P. Wise, D. Boussaoud, P.B. Johnson, R. Caminiti, Premotor and parietal cortex: corticocortical connectivity and combinatorial computations, Annu. Rev. Neurosci. 20 (1997) 25–42.

Erhan Oztop received his M.S. degree from Middle East Technical University in 1996; his Ph.D. degree from the University of Southern California in 2002. From 2002 to 2003, he was a visiting Researcher at the Advanced Telecommunications Research Institute, Computational Neuroscience Laboratories, Kyoto, Japan. He is now a Researcher at Japan Science Technology, working for the ICORP Computational Brain Project, and he is still affiliated with Advanced Telecommunications Research Institute. His research interests include computational modeling of the brain mechanisms of action understanding and visuomotor transformations, human-robot interaction, robotics, machine learning and cognitive neuroscience.

Hiroshi Imamizu obtained his Ph.D. (Experimental Psychology, 1995) at the University of Tokyo, Japan. He worked in ATR Human Information Processing Research Laboratories in Kyoto from 1992 to 1996 as a Research Associate. From 1996 to 2001, he worked as a leader of Computational Psychology Group in KDB, ERATO, JST. From 2001 to 2004, he worked as a senior researcher in ATR Human Information Science Laboratories. Since 2004, he is the head of Department of Cognitive Neuroscience in ATR Computational Neuroscience Laboratories. His research interest is in human sensorimotor learning from psychological and computational points of view.

Gordon Cheng is the head of the Department of Humanoid Robotics and Computational Neuroscience, ATR Computational Neuroscience Laboratories, Kyoto, Japan. He is also the Group Leader for the newly initiated JST International Cooperative Research Project (ICORP), Computational Brain. Before taking up these positions, he held fellowships from the Center of Excellence (COE), Science, and Technology Agency (STA) of Japan. Both fellowships were taken at the Humanoid Interaction Laboratory, Intelligent Systems Division at the ElectroTechnical Laboratory (ETL), Japan. At ETL he played a major role in developing a completely integrated humanoid robotics system. He received a Ph.D. in Systems Engineering from the Department of Systems Engineering, The Australian National University. Bachelor and Master degrees in Computer Science from the University of Wollongong, Australia. He is a society member of the IEEE Robotics & Automation and Computer Society. He is on the editorial board of the International Journal of Humanoid Robotics.

UNCORRECTED PROOF

NEUCOM : 10288

ARTICLE IN PRESS

Mitsuo Kawato received the B.S. degree in physics from Tokyo University in 1976, the M.E. and Ph.D. degrees in biophysical engineering from Osaka University in 1978 and 1981, respectively. From 1981 to 1988 he was a faculty member and lecturer of Osaka University. From 1992 he became a department head of Department 3, ATR Human Information Processing Research Laboratories. From 2003, Director of ATR Computational Neuroscience Laboratories. From 2004, he has been jointly appointed as the Director of the Computational Brain Project, ICORP, JST. From 1996 to 2001 he was jointly appointed as a director of Kawato Dynamic Brain Project, ERATO, JST. He has been jointly appointed as visiting professor of Kanazawa Institute of Technology, Nara Institute of Science and Technology and Osaka University. For the last 15 years he has been working in computational neuroscience. He was awarded Yonezawa founder's medal memorial special award of the Institute of Electronics, Information and Communication Engineers in 1991, outstanding research award of the International Neural Network Society in 1992, Osaka Science Prize in 1993, 10th Tsukahara Naka-akira Memorial Award in 1996 and Tokizane Toshihiko memorial award. He is a governing board member of Japanese Society of Neuroscience and Japan Neural Network Society and Member of Executive Committee of International Association for the Study of Attention and Performance.

UNCORRECTED PROOF